IEEE Access
Multidisciplinary | Rapid Review | Open Access Journal

Received February 14, 2020, accepted March 15, 2020, date of publication March 19, 2020, date of current version March 31, 2020.

Digital Object Identifier 10.1109/ACCESS.2020.2981967

Downlink Power Optimization for Cell-Free Massive MIMO Over Spatially Correlated Rayleigh Fading Channels

JIAHUA QIU, KUI XU, (Member, IEEE), XIAOCHEN XIA, ZHEXIAN SHEN, AND WEI XIE
College of Communications Engineering, Army Engineering University of PLA, Nanjing 210007, China

Corresponding author: Kui Xu (lgdxxukui@sina.com)

This work was supported in part by the National Natural Science Foundation of China under Grant 61671472, Grant 61771486, and Grant 61901519, and in part by the Jiangsu Province Natural Science Foundation, China, under Grant BK20181335.

ABSTRACT Cell-free massive multiple-input multiple-output (mMIMO) is regarded as a promising technology in the future wireless communication. This paper aims to minimize the downlink power consumption of cell-free mMIMO system under the downlink rate constraints of users and the power constraints of per-antenna over spatially correlated Rayleigh fading channels. Firstly, this paper studies the performance of two different downlink transmission modes: non-coherent joint transmission and coherent joint transmission. Then, for the two transmission modes, the corresponding downlink power optimization model is established and an efficient power optimization algorithm is proposed based on the Lagrange multiplier (LM) method. Under the power optimization model, this paper analyzes the impact of different factors on the downlink power consumption of cell-free mMIMO system. Simulation results show that coherent joint transmission performs better than non-coherent joint transmission on spectral efficiency (SE) and energy efficiency (EE). In addition, under the same power control strategy, the downlink power consumption of cell-free mMIMO is much lower than co-located mMIMO. Moreover, the total transmission power decreases when more antennas are utilized at each access point (AP) or spatial correlation of channels becomes weak.

INDEX TERMS Cell-free mMIMO, energy efficiency, non-coherent joint transmission, coherent joint transmission, power optimization and spatial correlation.

I. INTRODUCTION

Massive multiple-input multiple-output (mMIMO) technology can provide services for multiple users simultaneously in the same time-frequency resource by deploying a large number of antennas at the base station and using beamforming technology [1]. The application of this technology not only makes the capacity of the traditional cellular network greatly improved, but also makes fifth-generation (5G) communication gradually progress from theoretical research to reality [2], [3]. However, with the further study of mMIMO technology, researchers have found that the inherent cell mode in traditional cellular networks makes the edge users more vulnerable to serious inter-cell interference, and the quality of service will be greatly affected [4]. In order to overcome the capacity limitations of the cell mode, cell-free mMIMO emerged as a new concept [5].

In cell-free mMIMO, a large number of access points (APs) equipped with single or multiple antennas provide services to all users at the same time by exploring local channel state information (CSI) and performing joint transmission [6]. APs transmit the received uplink data to the central processing center (CPU) through the backhaul link, and CPU sends the downlink data and the power control coefficient to APs. Through the backhaul link between APs and CPU, CPU can use a centralized processing method to efficiently allocate various resources, thereby greatly improving the quality of service for users [7].

Compared with conventional mMIMO, cell-free mMIMO breaks through the design concept of ''cell-centric''. By introducing a ''user-centric'' approach, all users can get better and more uniform services. Its advantages are mainly reflected in the following aspects:

The associate editor coordinating the review of this manuscript and approving it for publication was Wei Wang.

- In cell-free mMIMO, there is no cell boundary, so users can be served by all APs, which brings huge diversity gain to users.
- With the increase of AP density, the distance between the user and the AP is shortened. And the path loss is greatly reduced.
- Since APs are randomly distributed and the number of antennas per AP is limited, the size of the AP can be further reduced, making it easier to configure in certain space-constrained scenarios.

Based on the above advantages, cell-free mMIMO is very suitable for hot-spot scenarios such as railway stations, airports, stadiums, large shopping malls, and smart factories, which also provides a direction for the research of next-generation mobile communication networks [6]. It was shown in [5] that cell-free mMIMO can increase the users' rate several-folds compared with conventional small cell model by applying the matched filtering in the uplink and conjugate beamforming in the downlink. In addition to high spectral efficiency (SE), cell-free mMIMO can also play a significant role in reducing transmission power consumption [9].

With the concept of ''green communication'', how to further improve the energy efficiency (EE) of the system or reduce the power consumption has become a hot issue [8]. The authors in [9] proposed the power control strategy of cell-free mMIMO to improve the overall EE, and the AP selection strategy to further reduce the system's backhaul power consumption. A novel power control strategy was proposed in [10] for cell-free mMIMO system and the system EE was maximized by using the zero-forcing (ZF) precoding algorithm. In [11], the effect of hardware impairments on the EE of cell-free mMIMO had been studied, and it was concluded that the negative impact of hardware impairments can be eliminated by deploying more APs. It was shown in [12], [13] that the loss and error caused by hybrid beamforming and channel estimation can be compensated by applying power control strategy reasonably in millimeter-wave communication, thus improving the EE performance of cell-free mMIMO. The EE performance of cell-free mMIMO and cellular mMIMO in urban and rural scenarios were introduced in [14], simulation results showed that the EE of cell-free mMIMO is much better than that of the cellular mMIMO by applying max-min power control strategy.

Most of recent work on cell-free mMIMO considered coherent joint transmission, different APs must send the same data symbol to the same user [9]–[15]. The major difficult of coherent joint transmission is that all APs must keep strict phase-synchronization during downlink transmission [4]. In order to alleviate the difficulty of strict phase-synchronization in coherent transmission, researchers have proposed the concept of non-coherent joint transmission in the research on coordinated multipoint (CoMP) transmission and heterogeneous networks [18], [19]. In non-coherent joint transmission, different APs can send different data symbols to the same user, and there is no need for strict phase-synchronization and phase calibration between APs, which reduces the complexity of the system [21]–[23]. It can be seen that the advantage of coherent joint transmission lies in higher spectral efficiency, but the disadvantage lies in high synchronization requirements. The advantages of non-coherent joint transmission are that it does not require strict phase-synchronization and is easy to achieve balancing load [20]. Therefore, in addition to coherent joint transmission, it is also of practical significance to study the performance of cell-free mMIMO in non-coherent joint transmission.

In addition, in the existing articles about the EE of cell-free mMIMO, only the total power constraint of all transmission antennas at the AP have been considered [9]–[14]. Although this method is relatively simple in analysis, this kind of power constraint is often impractical in implementation [24]. In the actual deployment process of a multi-antenna AP, since each antenna has an independent power amplifier, it is often subject to the linear constraint of its own power amplifier [25]. Therefore, it is of great practical significance to study the effect of the per-antenna power constraints on the EE of cell-free mMIMO.

Based on the above analysis, we investigate the downlink performance of cell-free mMIMO in different scenarios and propose the corresponding transmission power optimization method. The main contributions of this paper are as follows:

- For non-coherent joint transmission and coherent joint transmission, we obtain the expressions for the downlink SE of cell-free mMIMO over the spatially correlated Rayleigh fading channels.
- Under the constraint of per-antenna power and the constraint of the user's SE, we have established downlink transmission power optimization models for non-coherent joint transmission and coherent joint transmission, respectively. These problems are solved efficiently using the Lagrange multiplier (LM) method and the bisection method.
- In the proposed power optimization model, we study the influence of various factors such as the number of antennas, the constraint of user's SE and channel correlation on the total downlink transmission power of cell-free mMIMO. And its performance is compared with co-located mMIMO.
- Finally, we obtain that cell-free mMIMO can save more downlink transmission power than co-located mMIMO, and coherent joint transmission can achieve better EE than non-coherent joint transmission.

The rest of this paper is organized as follows. In Section II, we model the channel model and uplink training of cell-free mMIMO. In Section III, we analyze the downlink SE of cell-free mMIMO under the non-coherent joint transmission scenario. Section IV optimizes the total downlink transmission power under the non-coherent joint transmission scenario. We analyze the downlink SE of cell-free mMIMO under the coherent joint transmission scenario in Section V. In Section VI, we optimize the total downlink transmission power under the coherent joint transmission scenario.

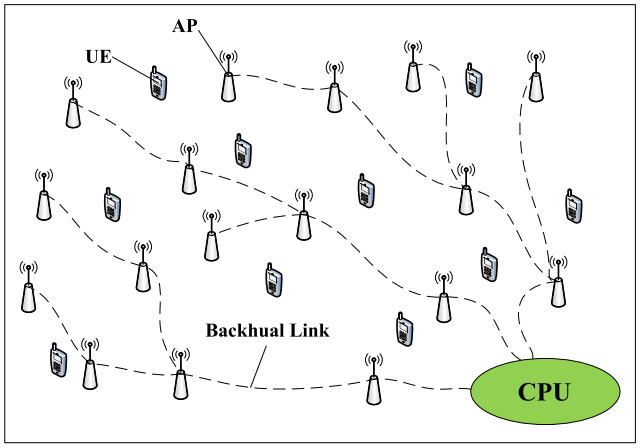

FIGURE 1. Cell-free mMIMO system.

The specific simulation results are given in Section VII. Finally, we summarize the full text in Section VIII.

Notation: Vectors and matrices are denoted with lowercase boldface and uppercase boldface, respectively. $\|\cdot\|$ denotes the Euclidean norm. $\mathbb{E}\{\cdot\}$ and $|\cdot|$ denote expectation and absolute value, respectively. $[\cdot]^T$, $[\cdot]^H$ and $\mathrm{tr}(\cdot)$ denote the transpose operator, conjugate operator and trace operator, respectively.

II. SYSTEM MODEL

A. CHANNEL MODEL

We consider a cell-free mMIMO model where L APs simultaneously serve K users in the same time-frequency resource. Each user has a single antenna, each AP has N antennas, and all APs are connected to CPU through backhaul link, see Fig. 1. In addition, we assume that the system is work in time-division duplex (TDD) mode. The length of a TDD block is τ_c, where the length τ_d for downlink data transmission and the length $\tau_p = \tau_c - \tau_d$ for pilot sequences transmission. And $\mathbf{h}_{kl} \in \mathbb{C}^{N\times 1}$ denotes the channel vector between the k-th user and the l-th AP.

This paper considers the spatially correlated Rayleigh fading channel model [16], which can be expressed as

$$\mathbf{h}_{kl} \sim \mathcal{CN}(\mathbf{0}_N, \mathbf{R}_{kl}) \tag{1}$$

where $\mathbf{R}_{kl} = \mathbb{E}\left\{\mathbf{h}_{kl}\mathbf{h}_{kl}^H\right\}$and $\mathbf{R}_{kl} \in \mathbb{C}^{N\times N}$ denotes the spatial correlation matrix for describing channel spatial correlation. Because the strong spatial correlation has the characteristics of large eigenvalue changes, we can know which directions are more likely to contain strong signal components from the spatial correlation matrix $\mathbf{R}_{kl}$.

For the spatial correlation matrix $\mathbf{R}_{kl}$, we apply the local scattering model based on Gaussian angular distribution [16]. The (m, n)th element of $\mathbf{R}_{kl}$ can be calculated as

$$[\mathbf{R}_{kl}]_{m,n} = \beta_{kl}\int_{-20\sigma_\phi}^{20\sigma_\phi} e^{2\pi j d_H(m-n)\sin(\phi+\delta)}\frac{1}{\sqrt{2\pi}\sigma_\phi}e^{-\frac{\delta^2}{2\sigma_\phi^2}}d\delta \tag{2}$$

where ϕ is the standard angle, representing the incident angle of the line of sight (LOS) path from user to AP, and β_{kl} denotes the large-scale fading coefficient. $d_H = \lambda/2$ denotes the antenna spacing, where λ denotes the carrier wavelength. $\delta \sim \mathcal{N}\left(0, \sigma_\phi^2\right)$ is the deviation between the incident angle of different paths and the standard angle. And σ_ϕ denotes the angular standard deviation (ASD). It can be seen from (2) that as σ_ϕ increases, the spatial correlation of the channel gradually decreases.

B. UPLINK TRAINING

Suppose that there are τ_p mutually orthogonal pilot sequences, which are respectively expressed as $\sqrt{\tau_p}\boldsymbol{\varphi}_1$, $\sqrt{\tau_p}\boldsymbol{\varphi}_2, \cdots, \sqrt{\tau_p}\boldsymbol{\varphi}_{\tau_p}$, where $\left\|\boldsymbol{\varphi}_t\right\|^2 = 1$ and $\boldsymbol{\varphi}_t \in \mathbb{C}^{\tau_p\times 1}$, $\forall t \in \{1, \cdots, \tau_p\}$. The pilot used by the k-th user is denoted as $\sqrt{\tau_p}\boldsymbol{\varphi}_{t_k}$, where $t_k \in \left\{1, 2, \cdots, \tau_p\right\}$ is the pilot index of the k-th user. The subset of users with the same pilot as the k-th user is denoted as $A_k \subset \{1, 2, \cdots, K\}$.

When all users transmit their pilot signals, the pilot signal received by the l-th AP is

$$\mathbf{y}_l^p = \sum_{i=1}^{K}\sqrt{\rho_i\tau_p}\mathbf{h}_{il}\boldsymbol{\varphi}_{t_i}^{\mathrm{T}} + \mathbf{N}_l \tag{3}$$

where ρ_i denotes the uplink pilot power of the i-th user, $\mathbf{N}_l \in \mathbb{C}^{N\times\tau_p}$ denotes the received noise matrix with independent and identically distributed $\mathcal{CN}(0, \sigma^2)$ components. And σ^2 denotes the noise power.

In order to estimate channel $\mathbf{h}_{kl}$, the l-th AP first multiple the normalized pilot signal $\boldsymbol{\varphi}_{t_k}$ with the received signal $\mathbf{y}_l^p$, and the processed received pilot signal can be expressed as

$$\begin{aligned}\mathbf{y}_{t_k l}^p &= \mathbf{y}_l^p\boldsymbol{\varphi}_{t_k}^* \\ &= \sum_{i=1}^{K}\sqrt{\rho_i\tau_p}\mathbf{h}_{il}\boldsymbol{\varphi}_{t_i}^{\mathrm{T}}\boldsymbol{\varphi}_{t_k}^* + \mathbf{N}_l\boldsymbol{\varphi}_{t_k}^* \\ &= \sum_{i\in A_k}\sqrt{\rho_i\tau_p}\mathbf{h}_{il} + \mathbf{N}_l\boldsymbol{\varphi}_{t_k}^*\end{aligned} \tag{4}$$

Then, according to channel estimation method in [16], we can get the minimum mean square error (MMSE) estimation of $\mathbf{h}_{kl}$ as

$$\hat{\mathbf{h}}_{kl} = \sqrt{\rho_k\tau_p}\mathbf{R}_{kl}\boldsymbol{\Psi}_{t_k l}^{-1}\mathbf{y}_{t_k l}^p = \mathbf{U}_{kl}\boldsymbol{\Psi}_{t_k l}^{-1}\mathbf{y}_{t_k l}^p \tag{5}$$

where $\boldsymbol{\Psi}_{t_k l} = \mathbb{E}\left\{\mathbf{y}_{t_k l}^p\left(\mathbf{y}_{t_k l}^p\right)^{\mathrm{H}}\right\} = \sum_{i\in A_k}\tau_p\rho_i\mathbf{R}_{il} + \mathbf{I}_N$ represents the correlation matrix of the received signal, and $\mathbf{U}_{kl} = \sqrt{\rho_k\tau_p}\mathbf{R}_{kl}$.

The channel estimation error is denoted as $\tilde{\mathbf{h}}_{kl} = \mathbf{h}_{kl} - \hat{\mathbf{h}}_{kl}$, which follows the normal distribution $\mathcal{CN}(\mathbf{0}_N, \mathbf{C}_{kl})$. The estimation error covariance matrix is as follows

$$\begin{aligned}\mathbf{C}_{kl} = \mathbb{E}\left\{\tilde{\mathbf{h}}_{kl}\tilde{\mathbf{h}}_{kl}^H\right\} &= \mathbf{R}_{kl} - \rho_k\tau_p\mathbf{R}_{kl}\boldsymbol{\Psi}_{t_k l}^{-1}\mathbf{R}_{kl} \\ &= \mathbf{R}_{kl} - \mathbf{U}_{kl}\boldsymbol{\Psi}_{t_k l}^{-1}\mathbf{U}_{kl}\end{aligned} \tag{6}$$

And according to [16], the MMSE estimate $\hat{\mathbf{h}}_{kl}$ and the estimation error $\tilde{\mathbf{h}}_{kl}$ are mutually independent.

III. NON-COHERENT DOWNLINK JOINT TRANSMISSION

In this section, we assume that non-coherent joint transmission is used in cell-free mMIMO, that is, different APs send different symbols to the same user, thereby alleviating phase-synchronization problems between APs.

A. NON-COHERENT DOWNLINK DATA TRANSMISSION

Assuming that the downlink signal sent by the l-th AP to the i-th user is s_{il}, which follows a normal distribution. And $s_{il} \sim \mathcal{CN}(0, p_{il})$, where p_{il} represents the downlink transmission power of the l-th AP to the i-th user. It can be obtained that the sending signal of the l-th AP is

$$\mathbf{x}_l = \sum_{i=1}^{K} \mathbf{w}_{il} s_{il}, \quad \forall l = 1, \cdots, L \tag{7}$$

where $\mathbf{w}_{il} \in \mathbb{C}^{N\times 1}$ represents the precoding vector of l-th AP to the i-th user.

According to the transmitted signal $\mathbf{x}_l$, we can get the received signal of the k-th user as

$$y_k^d = \sum_{l=1}^{L} \mathbf{h}_{kl}^H \mathbf{w}_{kl} s_{kl} + \sum_{i=1, i\neq k}^{K} \sum_{l=1}^{L} \mathbf{h}_{kl}^H \mathbf{w}_{il} s_{il} + n_k \tag{8}$$

where $n_k \sim \mathcal{CN}\left(0, \sigma_k^2\right)$ represents the received noise of the k-th user.

B. DOWNLINK SPECTRAL EFFICIENCY

After receiving the signals sent by all L APs, in order to detect the signals sent by different APs, the k-th user needs to use successive interference cancellation technology [21]–[23]. The specific idea is that the user first detects the signal sent by the first AP, and treats the remaining signal as interference. By analogy, the user detects the signal sent by the l-th AP, and regards the signal sent from the $(l+1)$-th AP to the L-th AP as interference, thus detecting the signal s_{kl}. Through successive interference cancellation technology, we can obtain the downlink SE and signal-to-interference and noise ratio (SINR) of the k-th user as follows

$$\mathrm{SE}_k^d = \frac{\tau_d}{\tau_c} \log_2\left(1 + \mathrm{SINR}_k^d\right) \tag{9}$$

$$\mathrm{SINR}_k^d = \frac{\sum_{l=1}^{L} p_{kl} \left|\mathbb{E}\left\{\mathbf{h}_{kl}^H \mathbf{w}_{kl}\right\}\right|^2}{\sum_{i=1}^{K}\sum_{l=1}^{L} p_{il}\mathbb{E}\left\{\left|\mathbf{h}_{kl}^H \mathbf{w}_{il}\right|^2\right\} - \sum_{l=1}^{L} p_{kl}\left|\mathbb{E}\left\{\mathbf{h}_{kl}^H \mathbf{w}_{kl}\right\}\right|^2 + \sigma_k^2} \tag{10}$$

The proof of (10) is given in Appendix A.

Remark: In this paper, we have mainly considered the following for non-coherent downlink transmission:

1) Non-coherent downlink transmission is a transmission method relative to coherent downlink transmission. The strategy used may be NOMA or other transmission technologies.
2) In the downlink transmission, since the CPU has completed power allocation, the power allocation result will have an impact on the calculation of SINR.
3) We do not consider the effect of the power allocation result on the order of successive interference cancellation. If NOMA technology is used, the power allocation will affect the AP sequencing.

Theorem 1: In the case of non-coherent downlink joint transmission, by using conjugate beamforming precoding, that is, $\mathbf{w}_{kl} = \hat{\mathbf{h}}_{kl}$, the downlink SINR of the cell-free mMIMO system is given in (11) at the bottom of this page.

Proof: Please see Appendix B.

IV. THE POWER OPTIMIZATION FOR NON-COHERENT JOINT TRANSMISSION

A. TOTAL DOWNLINK TRANSMISSION POWER

According to [9], we can get the downlink transmission power consumption model of cell-free mMIMO as follows

$$P_{total} = \sum_{l=1}^{L} P_l \tag{12}$$

where P_l represents the transmission power consumed by the l-th AP.

The average transmission power consumed by the l-th AP is

$$\begin{aligned} P_l &= \frac{1}{\alpha_l}\mathbb{E}\left\{\|\mathbf{x}_l\|^2\right\} = \frac{1}{\alpha_l}\sum_{i=1}^{K} p_{il}\mathbb{E}\left\{\|\mathbf{w}_{il}\|^2\right\} \\ &= \frac{1}{\alpha_l}\sum_{i=1}^{K} p_{il}\mathbb{E}\left\{\left\|\hat{\mathbf{h}}_{il}\right\|^2\right\} = \frac{1}{\alpha_l}\sum_{i=1}^{K} p_{il}\mathrm{tr}\left(\mathbf{U}_{il}\boldsymbol{\Psi}_{t_i l}^{-1}\mathbf{U}_{il}\right) \end{aligned} \tag{13}$$

where $0 < \alpha_l \leq 1$ is the efficiency of the power amplifier.

By substituting (13) into (12), and we can rewrite (12) as follows

$$P_{total} = \sum_{l=1}^{L}\frac{1}{\alpha_l}\sum_{i=1}^{K} p_{il}\mathrm{tr}\left(\mathbf{U}_{il}\boldsymbol{\Psi}_{t_i l}^{-1}\mathbf{U}_{il}\right) = \sum_{l=1}^{L}\frac{1}{\alpha_l}\sum_{i=1}^{K} p_{il}\eta_{il} \tag{14}$$

where $\eta_{il} = \mathrm{tr}\left(\mathbf{U}_{il}\boldsymbol{\Psi}_{t_i l}^{-1}\mathbf{U}_{il}\right)$.

$$\mathrm{SINR}_k^d = \frac{\sum_{l=1}^{L} p_{kl}\left|\mathrm{tr}\left(\mathbf{U}_{kl}\boldsymbol{\Psi}_{t_k l}^{-1}\mathbf{U}_{kl}\right)\right|^2}{\sum_{i=1}^{K}\sum_{l=1}^{L} p_{il}\mathrm{tr}\left(\mathbf{U}_{il}\boldsymbol{\Psi}_{t_i l}^{-1}\mathbf{U}_{il}\mathbf{R}_{kl}\right) + \sum_{l=1}^{L} p_{kl}\left\{\mathbb{E}\left\{\left\|\hat{\mathbf{h}}_{kl}\right\|^4\right\} - \mathrm{tr}\left(\left[\mathbf{U}_{kl}\boldsymbol{\Psi}_{t_k l}^{-1}\mathbf{U}_{kl}\right]^2\right) - \left|\mathrm{tr}\left(\mathbf{U}_{kl}\boldsymbol{\Psi}_{t_k l}^{-1}\mathbf{U}_{kl}\right)\right|^2\right\} + \sigma_k^2} \tag{11}$$

B. DOWNLINK SPECTRAL EFFICIENCY CONSTRAINTS

In the actual communication process, in order to enable all users to get good and fair service, it is necessary for each user's downlink rate to meet certain quality of service requirements. Therefore, this paper takes the minimum SE of user's downlink transmission as a measure of its quality of service. It can be obtained that the SE constraint that the k-th user needs to meet is given as follows

$$\mathrm{SE}_k^d = \frac{\tau_d}{\tau_c}\log_2\left(1+\mathrm{SINR}_k^d\right) \geq \mu_k, \quad \forall k = 1, \cdots, K \tag{15}$$

and the downlink SINR is limited as follows

$$\mathrm{SINR}_k^d \geq 2^{\frac{\tau_c}{\tau_d}\mu_k} - 1 \tag{16}$$

where μ_k represents the minimum SE required by the k-th user.

Let $\xi_{k,i,l} = \mathrm{tr}\left(\mathbf{U}_{il}\boldsymbol{\Psi}_{t_il}^{-1}\mathbf{U}_{il}\mathbf{R}_{kl}\right)$, $\chi_{kl} = \mathbb{E}\left\{\left\|\hat{\mathbf{h}}_{kl}\right\|^4\right\} - \mathrm{tr}\left(\left[\mathbf{U}_{kl}\boldsymbol{\Psi}_{t_kl}^{-1}\mathbf{U}_{kl}\right]^2\right) - \left|\mathrm{tr}\left(\mathbf{U}_{kl}\boldsymbol{\Psi}_{t_kl}^{-1}\mathbf{U}_{kl}\right)\right|^2$, and further simplify (11), then we can get the SINR of the k-th user as

$$\mathrm{SINR}_k^d = \frac{\sum_{l=1}^{L} p_{kl}\eta_{kl}^2}{\sum_{i=1}^{K}\sum_{l=1}^{L} p_{il}\xi_{k,i,l} + \sum_{l=1}^{L} p_{kl}\chi_{kl} + \sigma_k^2} \tag{17}$$

Then let $\tilde{\mu}_k = 2^{\frac{\tau_c}{\tau_d}\mu_k} - 1$, and bring (17) into (16). After simplification, we can get the downlink SE constraint of the k-th user as follows

$$\frac{1}{\tilde{\mu}_k}\sum_{l=1}^{L} p_{kl}\eta_{kl}^2 - \sum_{l=1}^{L} p_{kl}\chi_{kl} - \sum_{i=1}^{K}\sum_{l=1}^{L} p_{il}\xi_{k,i,l} - \sigma_k^2 \geq 0 \tag{18}$$

C. PER-ANTENNA POWER CONSTRAINTS

Due to cost considerations when designing the antenna, its power amplifier can only amplify the signal within a certain power range. If it exceeds this power range, the signal will have serious distortion. Therefore, in actual use, it is often necessary to set the power constraint of an antenna to ensure that the signal will not be distorted due to excessive transmission power.

In this paper, we consider the per-antenna power constraints, i.e.,

$$\frac{1}{\alpha_l}\sum_{i=1}^{K} p_{il}\mathbb{E}\left\{\left|[\mathbf{w}_{il}]_n\right|^2\right\} \leq \gamma_{l,n}, \quad \forall l; n \tag{19}$$

where $[\mathbf{w}_{il}]_n$ represents the n-th element in the precoding vector $\mathbf{w}_{il}$, $\gamma_{l,n}$ represents the power threshold of per-antenna. The left side of the inequality represents the average transmission power of the n-th antenna in the l-th AP.

Let $g_{i,l,n} = \mathbb{E}\left\{\left|\left[\hat{\mathbf{h}}_{il}\right]_n\right|^2\right\}$ and bring it to (19), the new power constraints can be obtained as follows

$$\frac{1}{\alpha_l}\sum_{i=1}^{K} p_{il}\mathbb{E}\left\{\left|[\mathbf{w}_{il}]_n\right|^2\right\} = \frac{1}{\alpha_l}\sum_{i=1}^{K} p_{il}\mathbb{E}\left\{\left|\left[\hat{\mathbf{h}}_{il}\right]_n\right|^2\right\} = \frac{1}{\alpha_l}\sum_{i=1}^{K} p_{il}g_{i,l,n} \leq \gamma_{l,n} \tag{20}$$

D. DOWNLINK TOTAL TRANSMISSION POWER OPTIMIZATION

According to (14), (18), (20), we can get the power optimization problem of non-coherent downlink transmission, which is to minimize the total downlink transmission power of the system on the premise of satisfying SE constraints and per-antenna power constraints. The power optimization model is as follows

$$\begin{aligned}
&\min_{p_{il}} \; P_{total} = \sum_{l=1}^{L}\frac{1}{\alpha_l}\sum_{i=1}^{K} p_{il}\eta_{il} \\
&s.t. \; \sum_{l=1}^{L} p_{kl}\left(\frac{\eta_{kl}^2}{\tilde{\mu}_k} - \chi_{kl}\right) - \sum_{i=1}^{K}\sum_{l=1}^{L} p_{il}\xi_{k,i,l} - \sigma_k^2 \geq 0 \quad \forall k \\
&\gamma_{l,n} - \frac{1}{\alpha_l}\sum_{i=1}^{K} p_{il}g_{i,l,n} \geq 0 \quad \forall l, n
\end{aligned} \tag{21}$$

In the above model, it is assumed that η_{il}, χ_{kl}, $\xi_{k,i,l}$ and $g_{i,l,n}$ can be obtained from statistical CSI. Therefore, the problem (21) can be regarded as minimizing the total transmission power of the system by optimizing the downlink transmission power p_{il}.

In (21), the objective of optimization is a convex function, and the constraints are all linear functions. According to the definition of convex optimization [17], the power optimization problem is a standard convex optimization problem. Because all of the inequality constraints are affine functions, according to Slatter's theory [26], the karush-kuhn-tucker (KKT) condition is a necessary and sufficient condition for the optimal solution of problem (21). For solving the problem (21), we can use the KKT optimality conditions and the LM method following a procedure similar to [26]. The optimal power allocation scheme is given in **Algorithm 1**. A application of **Algorithm 1** is given in Appendix C.

V. COHERENT DOWNLINK JOINT TRANSMISSION

In this section, we assume that the downlink transmission of cell-free mMIMO adopts coherent joint transmission, that is, different APs send the same signal to the same user, and the APs meet the phase-synchronization requirements.

A. COHERENT DOWNLINK DATA TRANSMISSION

Supposing that the downlink signal sent by the l-th AP to the i-th user is $s_{il} = \sqrt{p_{il}}q_i$, which obeys the normal distribution $\mathcal{CN}(0, p_{il})$. p_{il} denotes the downlink transmission power, and q_i denotes the symbol sent to the i-th user. The sending signal of the l-th AP is

$$x_l = \sum_{i=1}^{K}\mathbf{w}_{il}s_{il} \tag{22}$$

The received signal of the k-th user is

$$\begin{aligned}
y_k^d &= \sum_{l=1}^{L}\mathbf{h}_{kl}^H\mathbf{w}_{kl}s_{kl} + \sum_{i=1,i\neq k}^{K}\sum_{l=1}^{L}\mathbf{h}_{kl}^H\mathbf{w}_{il}s_{il} + n_k \\
&= \sum_{l=1}^{L}\sqrt{p_{kl}}\mathbf{h}_{kl}^H\mathbf{w}_{kl}q_k + \sum_{i=1,i\neq k}^{K}\sum_{l=1}^{L}\sqrt{p_{il}}\mathbf{h}_{kl}^H\mathbf{w}_{il}q_i + n_k
\end{aligned} \tag{23}$$

Algorithm 1 Downlink Power Allocation for (21)

1. Input: the number of users K, the number of APs L, the number of antennas N;

2. Initialization: $count = 1$; $temp = 0$; $T = \binom{K+L\times N}{K\times L}$

3. Finding the Optimal Power Allocation Solution

If $K + L \times N > K \times L$

Determine the T feasible LM realizations from (22);

while $count \leq T$ or $temp == 0$ **do**

Sovle $K \times L$ equalities for $count$-th realizations of the LMs, and we can get the power allocation solution p_{kl};

if p_{kl} satisfies the remaining $K + L \times N$ inequalities

then p_{kl} is the optimal solution; $temp = 1$;

else $count = count + 1$;

end if

end while

Else

Determine the $2^{K+L\times N}$ feasible LM realizations from (22), and assume that in $count$-th realizations of the LMs, the number of non-zero Lagrangian multipliers is S;

while count $\leq 2^{K+L\times N}$ or $temp == 0$ **do**

Solve $S + K \times L$ equalities for $count$-th realizations of the LMs, and we can get the power allocation solution p_{kl};

if p_{kl} satisfies the remaining $K + L \times N - S$ inequalities

then p_{kl} is the optimal solution; $temp = 1$;

else $count = count + 1$;

end if

end while

End If

B. DOWNLINK SPECTRAL EFFICIENCY

In order to obtain the SE of the user in the coherent downlink transmission, we rewrite the downlink received signal of the k-th user as

$$y_k^d = \mathrm{DS}_k \cdot q_k + \mathrm{BU}_k \cdot q_k + \sum_{i\neq k}^{K} \mathrm{UI}_{ki} \cdot q_i + n_k \tag{24}$$

where

$$\mathrm{DS}_k = \mathbb{E}\left\{\sum_{l=1}^{L} \sqrt{p_{kl}}\mathbf{h}_{kl}^H \mathbf{w}_{kl}\right\} \tag{25}$$

$$\mathrm{BU}_k = \sum_{l=1}^{L} \sqrt{p_{kl}}\mathbf{h}_{kl}^H \mathbf{w}_{kl} - \mathbb{E}\left\{\sum_{l=1}^{L} \sqrt{p_{kl}}\mathbf{h}_{kl}^H \mathbf{w}_{kl}\right\} \tag{26}$$

$$\mathrm{UI}_{ki} = \sum_{l=1}^{L} \sqrt{p_{il}}\mathbf{h}_{kl}^H \mathbf{w}_{il} \tag{27}$$

denote the desired signal (DS), the beamforming uncertainty gain (BU) and multiuser interference (UI), respectively.

According to the existing results of information theory [16], we can get the downlink SINR of the k-th user as

$$\mathrm{SINR}_k^d = \frac{|\,\mathrm{DS}_k|^2}{\mathbb{E}\left\{|\mathrm{BU}_k|^2\right\} + \sum_{i=1,i\neq k}^{K} \mathbb{E}\left\{|\,\mathrm{UI}_{ki}|^2\right\} + \sigma_k^2} \tag{28}$$

Substituting (25), (26), and (27) into (28), the simplified SINR expression can be obtained as follows

$$\mathrm{SINR}_k^d = \frac{\left|\mathbb{E}\left\{\sum_{l=1}^{L} \sqrt{p_{kl}}\mathbf{h}_{kl}^H \mathbf{w}_{kl}\right\}\right|^2}{\sum_{i=1}^{K} \mathbb{E}\left\{\left|\sum_{l=1}^{L} \sqrt{p_{il}}\mathbf{h}_{kl}^H \mathbf{w}_{il}\right|^2\right\} - \left|\mathbb{E}\left\{\sum_{l=1}^{L} \sqrt{p_{kl}}\mathbf{h}_{kl}^H \mathbf{w}_{kl}\right\}\right|^2 + \sigma_k^2} \tag{29}$$

where the proof of (29) is given in Appendix D.

Theorem 2: In the case of coherent downlink joint transmission, by using conjugate beamforming precoding, the downlink SINR of the k-th user can be obtained as (30), shown at the bottom of the next page.

Proof: Please see Appendix E.

VI. THE POWER OPTIMIZATION FOR COHERENT JOINT TRANSMISSION

A. DOWNLINK SPECTRAL EFFICIENCY CONSTRAINTS

If η_{il}, χ_{kl} and $\xi_{k,i,l}$ are introduced into (30) and further simplified, the SINR of the k-th user can be obtained as follows

$$\mathrm{SINR}_k^d = \frac{\left|\sum_{l=1}^{L} \sqrt{p_{kl}}\eta_{kl}\right|^2}{\sum_{i=1}^{K}\sum_{l=1}^{L} p_{il}\xi_{k,i,l} + \sum_{l=1}^{L} p_{kl}\chi_{kl} + \sigma_k^2} \tag{31}$$

By introducing $\tilde{\mu}_k$ and (31) into (16), we can get the downlink SE constraints of the k-th user as follows

$$\frac{1}{\tilde{\mu}_k}\left|\sum_{l=1}^{L} \sqrt{p_{kl}}\eta_{kl}\right|^2 - \sum_{i=1}^{K}\sum_{l=1}^{L} p_{il}\xi_{k,i,l} - \sum_{l=1}^{L} p_{kl}\chi_{kl} - \sigma_k^2 \geq 0 \tag{32}$$

B. DOWNLINK TOTAL TRANSMISSION POWER OPTIMIZATION

Finally, according to (14), (20) and (32), we can get the downlink power optimization model under coherent joint transmission as follows

$$\begin{aligned} \min_{p_{il}} \ & P_{total} = \sum_{l=1}^{L} \frac{1}{\alpha_l} \sum_{i=1}^{K} p_{il}\eta_{il} \\ s.t. \ & \frac{1}{\tilde{\mu}_k}\left|\sum_{l=1}^{L} \sqrt{p_{kl}}\eta_{kl}\right|^2 - \sum_{i=1}^{K}\sum_{l=1}^{L} p_{il}\xi_{k,i,l} \\ & - \sum_{l=1}^{L} p_{kl}\chi_{kl} - \sigma_k^2 \geq 0 \quad \forall k \\ & \gamma_{l,n} - \frac{1}{\alpha_l} \sum_{i=1}^{K} p_{il} g_{i,l,n} \geq 0 \quad \forall l, n \end{aligned} \tag{33}$$

Since the first inequality constraint in (33) is not a standard linear function, the above problem is a quasi-convex problem. By rewriting the quasi-convex problem and letting $\theta_{il} = \sqrt{p_{il}}$, we can get the optimization problem as follows

$$\begin{aligned} \min_{\theta_{il}} \ & P_{total} = \sum_{l=1}^{L} \frac{1}{\alpha_l} \sum_{i=1}^{K} \theta_{il}^2 \eta_{il} \\ s.t. \ & \frac{1}{\sqrt{\tilde{\mu}_k}} \left| \sum_{l=1}^{L} \theta_{kl} \eta_{kl} \right| \geq \|\mathbf{z}_k\| \quad \forall k \\ & \gamma_{l,n} - \frac{1}{\alpha_l} \sum_{i=1}^{K} \theta_{il}^2 g_{i,l,n} \geq 0 \quad \forall l, n \end{aligned} \tag{34}$$

where $\mathbf{z}_k = \left[\bar{\mathbf{z}}_k, \tilde{\mathbf{z}}_k, \sigma_k\right]^T$, $\tilde{\mathbf{z}}_k = \left[\theta_{k1}\sqrt{\chi_{k1}}, \cdots, \theta_{kL}\sqrt{\chi_{kL}}\right]$, $\bar{\mathbf{z}}_k = \left[\theta_{11}\sqrt{\xi_{k,1,1}}, \cdots, \theta_{1L}\sqrt{\xi_{k,1,L}}, \cdots, \theta_{KL}\sqrt{\xi_{k,K,L}}\right]$.

Algorithm 2 Bisection Algorithm for Solving (34)

1) Initialization: select the initial variables $t_{\min}$ and $t_{\max}$ to determine the value range of the objective function in question (34). Choose tolerance $\delta > 0$.
2) Let $t = (t_{\min} + t_{\max})/2$ and use CVX to solve the following convex optimization problems.

$$\begin{cases} \sum_{l=1}^{L} \frac{1}{\alpha_l} \sum_{i=1}^{K} \theta_{il}^2 \eta_{il} \leq t \\ \|\mathbf{z}_k\| \leq \frac{1}{\sqrt{\tilde{\mu}_k}} \left| \sum_{l=1}^{L} \theta_{kl} \eta_{kl} \right|, & k = 1, \ldots, K \\ \frac{1}{\alpha_l} \sum_{i=1}^{K} \theta_{il}^2 g_{i,l,n} \leq \gamma_{l,n}, & l = 1, \ldots, L, \\ & n = 1, \ldots N \\ \theta_{il} \geq 0, & i = 1, \ldots, K, \\ & l = 1, \ldots, L \end{cases} \tag{35}$$

3) If there is a feasible solution in (35), then let $t_{\max} = t$, otherwise let $t_{\min} = t$.
4) If the condition $t_{\max} - t_{\min} < \delta$ is satisfied, this loop is exited, then θ_{il} and t are output. Otherwise, return to step (2) to continue the solution.

Since problem (34) is a second-order cone program (SOCP) problem [17], the convex optimization tool can be used to solve it, such as CVX [27]. To solve this problem, we use the bisection method in **Algorithm 2** to reduce the solution range of problem (34) and reduce its computational complexity. In **Algorithm 2**, we first use the bisection method to reduce problem (34) to the convex optimization problem (35). Then we use CVX to solve (35), and get the minimum transmission power and the optimal power allocation scheme. Combined with the bisection method, the solution algorithm is given in **Algorithm 2**.

VII. NUMERICAL RESULTS AND DISCUSSIONS

A. POWER OPTIMIZATION MODEL IN CO-LOCATED mMIMO

In order to compare with cell-free mMIMO, we perform the same power optimization in the co-located mMIMO model. It is assumed that there is only one base station in co-located mMIMO, the number of antennas M in the base station is the same as the total number of antennas in cell-free mMIMO. And other parameters are the same as the power optimization model of cell-free mMIMO. The downlink transmission power optimization models of co-located mMIMO during non-coherent joint transmission and coherent joint transmission are shown in (36) and (37), respectively.

$$\begin{aligned} \min_{p_{i0}} \ & P_{total} = \frac{1}{\alpha_0} \sum_{i=1}^{K} p_{i0} \eta_{i0} \\ s.t. \ & p_{k0} \left(\frac{\eta_{k0}^2}{\tilde{\mu}_k} - \chi_{k0} \right) - \sum_{i=1}^{K} p_{i0} \xi_{k,i,0} - \sigma_k^2 \geq 0 \quad \forall k \\ & \gamma_{0,n} - \frac{1}{\alpha_l} \sum_{i=1}^{K} p_{i0} g_{i,0,n} \geq 0 \quad \forall n \end{aligned} \tag{36}$$

$$\begin{aligned} \min_{p_{i0}} \ & P_{total} = \frac{1}{\alpha_0} \sum_{i=1}^{K} p_{i0} \eta_{i0} \\ s.t. \ & \frac{1}{\sqrt{\tilde{\mu}_k}} \left| \sqrt{p_{k0}} \eta_{k0} \right| \geq \|\mathbf{z}_k\| \quad \forall k \\ & \gamma_{0,n} - \frac{1}{\alpha_l} \sum_{i=1}^{K} p_{i0} g_{i,0,n} \geq 0 \quad \forall n \end{aligned} \tag{37}$$

where $\alpha_0, p_{i0}, \eta_{i0}, \mathbf{z}_k, \gamma_{0,n}$ and $g_{i,0,n}$ all represent related parameters in co-located mMIMO, and their meanings are the same as corresponding parameters in cell-free mMIMO.

B. PARAMETERS SETTING

Assuming that all APs and users are randomly distributed within 0.5×0.5 km^2 square range, and the downlink transmission adopts conjugate beamforming precoding [5]. Assuming that the uplink pilot length τ_p and the number of users K are the same, there is no pilot contamination in the system. And the efficiency of the power amplifier α_l is 0.4 in Fig. 2 - Fig. 5. We use Monte Carlo simulation method, the number of simulation is 1000.

$$\mathrm{SINR}_k^d = \frac{\sum_{l=1}^{L} p_{kl} \left| \mathrm{tr}\left(\mathbf{U}_{kl} \boldsymbol{\Psi}_{t_k l}^{-1} \mathbf{U}_{kl} \right) \right|^2}{\sum_{i=1}^{K} \sum_{l=1}^{L} p_{il} \mathrm{tr}\left(\mathbf{U}_{il} \boldsymbol{\Psi}_{t_i l}^{-1} \mathbf{U}_{il} \mathbf{R}_{kl} \right) + \sum_{l=1}^{L} p_{kl} \left\{ \mathbb{E}\left\{ \left\| \hat{\mathbf{h}}_{kl} \right\|^4 \right\} - \mathrm{tr}\left(\left[\mathbf{U}_{kl} \boldsymbol{\Psi}_{t_k l}^{-1} \mathbf{U}_{kl} \right]^2 \right) - \left| \mathrm{tr}\left(\mathbf{U}_{kl} \boldsymbol{\Psi}_{t_k l}^{-1} \mathbf{U}_{kl} \right) \right|^2 \right\} + \sigma_k^2} \tag{30}$$

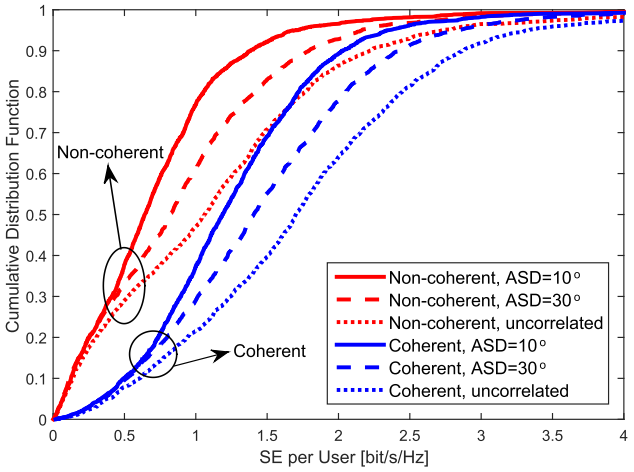

FIGURE 2. In coherent and non-coherent joint transmission scenarios, cumulative distribution of downlink SE for users in cell-free mMIMO. Here, $N = 4$, $K = 10$, $L = 40$, and $M = 160$.

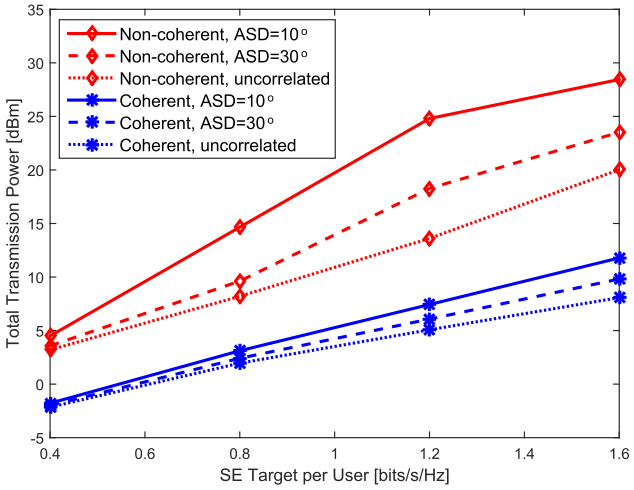

FIGURE 3. In coherent and non-coherent joint transmission scenarios, as the user's target SE changes, the spatial correlation in cell-free mMIMO affects its total downlink transmission power. Here, $N = 4$, $K = 10$, $L = 40$, and $M = 160$.

The large-scale fading model [16] applied in this paper is expressed as

$$\beta_{kl}\,[\mathrm{dB}] = -30.5 - 36.7\log_{10}\left(\frac{d_{kl}}{1\mathrm{m}}\right) + F_{kl} \qquad (38)$$

where d_{kl} denotes the distance between the k-th user and the l-th AP, and $F_{kl} \sim \mathcal{N}\left(0, 4^2\right)$ denotes the shadow fading.

Because the simulation parameters of each figure will be different, most of the general parameters will be given in Table 1, and the specific parameters of each figure will be given in the diagram and discussion.

C. SIMULATION RESULTS

In Fig. 2, we compare the SE differences between non-coherent and coherent transmission for cell-free mMIMO under different channel correlations. In the figure, ASD = 10°represents strong spatially correlated channels, ASD = 30°represents weak spatially correlated channels, and

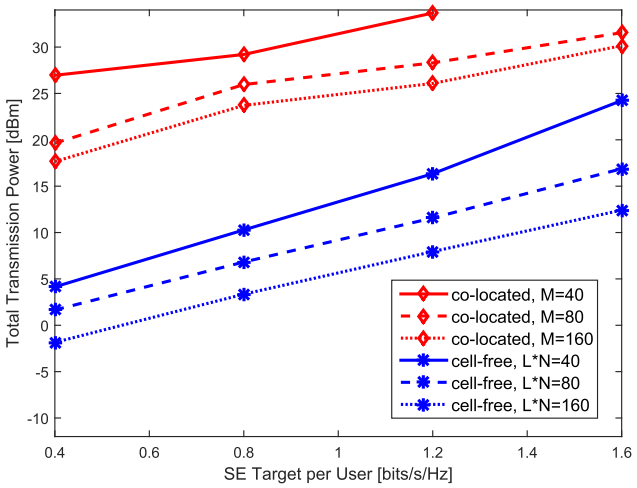

FIGURE 4. In coherent joint transmission, the total transmission power versus the SE target for cell-free mMIMO and co-located mMIMO under different antenna numbers. Here, $N = 1,2,4$, $K = 10$, $L = 40$, $M = L \times N$ and $ASD = 10^\circ$.

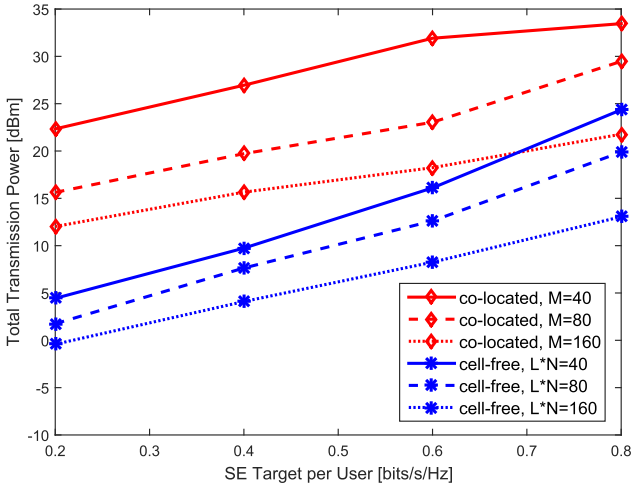

FIGURE 5. In non-coherent joint transmission, the total transmission power versus the SE target for cell-free mMIMO and co-located mMIMO under different antenna numbers. Here, $N = 1,2,4$, $K = 10$, $L = 40$, $M = L \times N$ and $ASD = 10^\circ$.

TABLE 1. Setting of simulation parameters.

Symbol	Meaning	Value
$\gamma_{l,n}$	The power constraint of per-antenna	50 mW
ρ_i	The uplink pilot power	200 mW
σ_k^2	Noise power	-96 dBm
τ_c	The length of coherent block	200
B	Bandwidth	20 MHz
f	The carrier frequency	1.9 GHz
L	The number of APs	40

uncorrelated represents spatially uncorrelated channels. Here we do not consider the problem of power optimization, and assuming that the AP allocates the same power to all users, which is 50 mW. It can be seen that under the same spatial correlation, the cumulative distribution function (CDF) curve of coherent transmission is located on the right side of the non-coherent transmission curve, which indicates that the

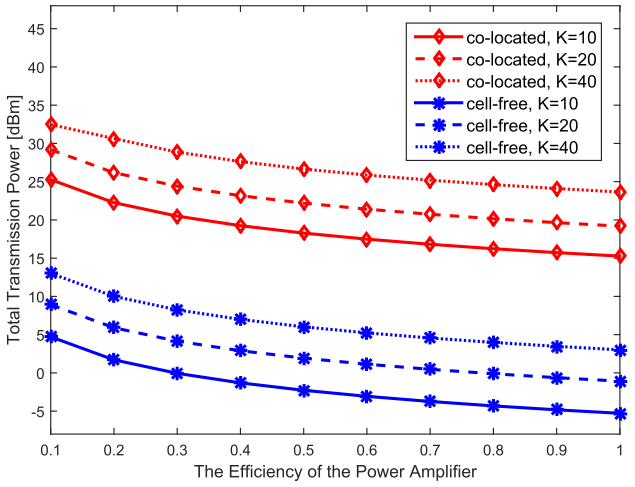

FIGURE 6. In coherent joint transmission, the total transmission power versus the efficiency of the power amplifier for cell-free mMIMO and co-located mMIMO under different user numbers. Here, $N = 4$, $K = 10,20,40$, $L = 40$, $M = 160$ and $ASD = 10^{\circ}$.

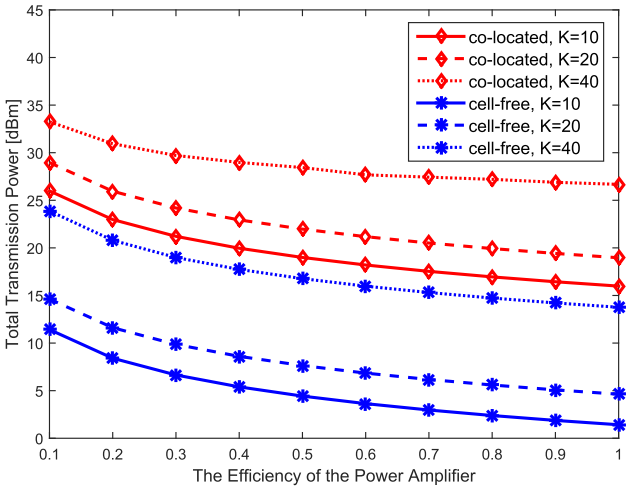

FIGURE 7. In non-coherent joint transmission, the total transmission power versus the efficiency of the power amplifier for cell-free mMIMO and co-located mMIMO under different user numbers. Here, $N = 4$, $K = 10,20,40$, $L = 40$, $M = 160$ and $ASD = 10^{\circ}$.

probability of obtaining high SE by the coherent joint transmission method is greater than that of the non-coherent joint transmission. Therefore, Fig. 2 indicates that coherent joint transmission is superior to non-coherent joint transmission in terms of SE. In addition, with the decrease of spatial correlation, the CDF curve of the user's SE is shifted to the right, that is, the probability of the user obtaining high SE is gradually increasing. This shows that the cell-free mMIMO system performs transmission under weak spatial correlation, which is beneficial to improving the user's SE.

Fig. 3 shows that the power consumption differences between non-coherent and coherent transmission for cell-free mMIMO under different channel correlations. It can be seen that under the same user's target rate, the power consumption of coherent joint transmission is about 5-15 dBm less than that of non-coherent joint transmission, indicating that the coherent joint transmission is more conducive to reducing energy. As can be seen that when SE target = 1.2 bit/s/Hz, for non-coherent joint transmission, the uncorrelated channel can save about 12 dBm of power than the strongly correlated channel. For coherent joint transmission, the difference in power consumption is less than 5 dBm. This indicates that for coherent joint transmission, the channel spatial correlation has little effect on its power consumption. However, for non-coherent joint transmission, the influence of channel spatial correlations on the power consumption is more obvious. The reason is that cell-free mMIMO can achieve higher downlink SE when transmitting on spatially uncorrelated channels.

In Fig. 4 and Fig. 5, we compare the total transmission power of cell-free mMIMO and co-located mMIMO under different user's SE constraints with the change of antenna number. Fig. 4 shows that in the coherent joint transmission scenario, the total downlink power consumption of cell-free mMIMO and co-located mMIMO keeps a growth relationship with the increase of user's target rate. This shows that the selection of the user's target rate has a greater impact on the total transmission power consumption. In addition, whether cell-free mMIMO and co-located mMIMO, the total downlink transmission power will decrease with the increase of the total number of antennas. This shows that under the same service conditions, more antennas are deployed in the AP, which is conducive to reducing the total downlink power consumption. Of course, this does not take into account factors such as the circuit's power consumption in the AP itself. Moreover, the total downlink transmission power required by cell-free mMIMO is much lower than that of co-located mMIMO, which can save about 10-20 dBm of power consumption. The conclusion in the non-coherent joint transmission scenario in Fig. 5 is basically the same as that in Fig. 4.

Fig. 6 and Fig. 7 depict that the influence of different user numbers and the efficiency of the power amplifier on the total downlink transmission power of cell-free mMIMO and co-located mMIMO. We assume that the SE constraint of each user is 0.5 bit/s/Hz. Fig. 6 shows that in the coherent joint transmission mode, with the improvement of the efficiency of power amplifier α_l, the downlink power consumption of cell-free mMIMO and co-located mMIMO shows a downward trend. And when $\alpha_l > 0.5$, the energy efficiency gain is gradually weakened. In addition, as the number of users increases, the transmission power consumed by the system also increases. In Fig. 7, the conclusions of cell-free mMIMO and co-located mMIMO in non-coherent downlink transmission are basically the same as those in Fig. 6. The biggest difference is that when $K = 40$, the transmission power consumption of the system will increase significantly. This indicates that under non-coherent joint transmission, the increase in the number of users has a greater impact on the power consumption.

D. ALGORITHM COMPLEXITY ANALYSIS

Because the problems solved by **Algorithm 1** and **Algorithm 2** are not the same, the complexity of the two

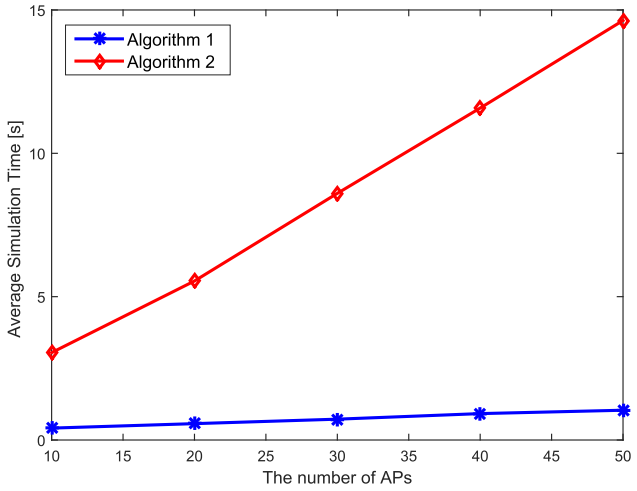

FIGURE 8. Average simulation time versus the number of APs for Algorithm 1 and Algorithm 2 under spatially uncorrelated channels. Here, $N = 4$, $K = 10$.

cannot be directly compared. Therefore, we compare the average simulation time of the two algorithms to analyze the complexity. Fig. 8 shows that the changes in the average simulation time of **Algorithm 1** and **Algorithm 2** as the number of APs changes. The simulation parameters are as follows: the computer's CPU is Intel Core i3-2350M, the memory is 4 GB, the number of simulations is 1000 times and the SE constraint of each user is 0.4 bit/s/Hz. As can be seen that the average simulation time of **Algorithm 2** is significantly higher than **Algorithm 1**. This shows that under the same conditions, the complexity of **Algorithm 2** is higher than **Algorithm 1**. In addition, with the increase in the number of APs, the average simulation time of both algorithms has increased to varying degrees. For **Algorithm 2**, when $L = 10$, the average simulation time is 3.048 s, and when $L = 50$, the average simulation time is 14.633 s, which is more than 4 times increase when compared with $L = 10$. For **Algorithm 1**, the growth rate is more than 2 times, which is smaller than **Algorithm 2**. This shows that the increase in the number of APs will significantly increase the complexity of **Algorithm 2**, and its influence on **Algorithm 2** is greater than that on **Algorithm 1**.

VIII. CONCLUSION

This paper investigates the total downlink transmission power optimization problem in cell-free mMIMO system with the antenna power constraints and the user's downlink rate constraints. Two power optimization schemes are proposed for the coherent joint transmission and non-coherent joint transmission scenarios. The results show that coherent joint transmission can save about 5-15 dBm of power consumption compared to non-coherent joint transmission in cell-free mMIMO. This indicates that even if non-coherent joint transmission is helpful to solve the phase-synchronization problem in cell-free mMIMO, from the perspective of user's rate and energy consumption, coherent joint transmission is still the better choice. In addition, simulation results also show that under the same user's target rate, cell-free mMIMO can save more energy than co-located mMIMO. And by deploying more antennas on the AP or controlling the number of users, the downlink transmission power of the system can be reduced. Finally, by analyzing the influence of spatial correlation, it can be seen that cell-free mMIMO requires more energy to be transmitted on spatially correlated channels than spatially uncorrelated channels.

APPENDIXES

APPENDIX A
PROOF OF (10)

Firstly, using successive interference cancellation technology [21]–[23], the k-th user detects that the signal sent by the first AP is

$$y_{k1}^{d} = \mathbb{E}\left\{\mathbf{h}_{k1}^{H}\mathbf{w}_{k1}\right\}s_{k1} + \left(\mathbf{h}_{k1}^{H}\mathbf{w}_{k1} - \mathbb{E}\left\{\mathbf{h}_{k1}^{H}\mathbf{w}_{k1}\right\}\right)s_{k1} + \sum_{l=2}^{L}\mathbf{h}_{kl}^{H}\mathbf{w}_{kl}s_{kl} + \sum_{i=1,i\neq k}^{K}\sum_{l=1}^{L}\mathbf{h}_{kl}^{H}\mathbf{w}_{il}s_{il} + n_k \quad (A.1)$$

Then, the k-th user separates the signal sent by the next AP from the remaining signals, and thus the signal sent by the j-th AP is

$$\begin{aligned} y_{kj}^{d} &= y_{k}^{d} - \sum_{l=1}^{j-1}\mathbb{E}\left\{\mathbf{h}_{kl}^{H}\mathbf{w}_{kl}\right\}s_{kl} \\ &= \mathbb{E}\left\{\mathbf{h}_{kj}^{H}\mathbf{w}_{kj}\right\}s_{kj} + \sum_{l=1}^{j}\left(\mathbf{h}_{kl}^{H}\mathbf{w}_{kl} - \mathbb{E}\left\{\mathbf{h}_{kl}^{H}\mathbf{w}_{kl}\right\}\right)s_{kl} \\ &\quad + \sum_{l=j+1}^{L}\mathbf{h}_{kl}^{H}\mathbf{w}_{kl}s_{kl} + \sum_{i=1,i\neq k}^{K}\sum_{l=1}^{L}\mathbf{h}_{kl}^{H}\mathbf{w}_{il}s_{il} + n_k \end{aligned} \quad (A.2)$$

where, $\mathbb{E}\left\{\mathbf{h}_{kj}^{H}\mathbf{w}_{kj}\right\}s_{kj}$ represents the desired signal and the remaining terms are uncorrelated noise, which is denoted with v_{kj}.

Thus, the SINR of the j-th AP transmitted signal demodulated by the k-th user is

$$\begin{aligned} \mathrm{SINR}_{kj}^{d} &= \frac{p_{kj}\left|\mathbb{E}\left\{\mathbf{h}_{kj}^{H}\mathbf{w}_{kj}\right\}\right|^{2}}{\mathbb{E}\left\{\left|v_{kj}\right|^{2}\right\}} \\ &= \frac{p_{kj}\left|\mathbb{E}\left\{\mathbf{h}_{kj}^{H}\mathbf{w}_{kj}\right\}\right|^{2}}{\sum_{i=1}^{K}\sum_{l=1}^{L}p_{il}\mathbb{E}\left\{\left|\mathbf{h}_{kl}^{H}\mathbf{w}_{il}\right|^{2}\right\} - \sum_{l=1}^{j}p_{kl}\mathbb{E}\left\{\left|\mathbf{h}_{kl}^{H}\mathbf{w}_{kl}\right|^{2}\right\} + \sigma_{k}^{2}} \end{aligned} \quad (A.3)$$

Combined with the above formula, we can get that the total downlink SE of the k-th user as follows (A.4), as shown at the bottom of the next page.

According to (A.4), so we can obtain (10).

APPENDIX B
PROOF OF THEOREM 1

By substituting $\mathbf{w}_{kl} = \hat{\mathbf{h}}_{kl}$ into (11), we can get

$$\mathrm{SINR}_k^d = \frac{\sum_{l=1}^{L} p_{kl}\left|\mathbb{E}\left\{\mathbf{h}_{kl}^H\hat{\mathbf{h}}_{kl}\right\}\right|^2}{\sum_{i=1}^{K}\sum_{l=1}^{L} p_{il}\mathbb{E}\left\{\left|\mathbf{h}_{kl}^H\hat{\mathbf{h}}_{il}\right|^2\right\} - \sum_{l=1}^{L} p_{kl}\left|\mathbb{E}\left\{\mathbf{h}_{kl}^H\hat{\mathbf{h}}_{kl}\right\}\right|^2 + \sigma_k^2} \tag{B.1}$$

For the numerator term in (B.1), we can get

$$\begin{aligned}&\left|\mathbb{E}\left\{\mathbf{h}_{kl}^H\hat{\mathbf{h}}_{kl}\right\}\right|^2\\ &= \left|\mathbb{E}\left\{\mathrm{tr}(\hat{\mathbf{h}}_{kl}\mathbf{h}_{kl}^H)\right\}\right|^2 = \left|\mathbb{E}\left\{\mathrm{tr}(\mathbf{U}_{kl}\boldsymbol{\Psi}_{t_kl}^{-1}\mathbf{y}_{t_kl}^p\mathbf{h}_{kl}^H)\right\}\right|^2\\ &= \left|\sqrt{\rho_k\tau_p}\mathrm{tr}\left(\mathbf{U}_{kl}\boldsymbol{\Psi}_{t_kl}^{-1}\mathbb{E}\left\{\mathbf{h}_{kl}\mathbf{h}_{kl}^H\right\}\right)\right|^2 = \left|\mathrm{tr}\left(\mathbf{U}_{kl}\boldsymbol{\Psi}_{t_kl}^{-1}\mathbf{U}_{kl}\right)\right|^2\end{aligned} \tag{B.2}$$

Then, for the first denominator term in (B.1), we need to discuss in two cases.

1) If $i = k$,

$$\begin{aligned}&\mathbb{E}\left\{\left|\mathbf{h}_{kl}^H\hat{\mathbf{h}}_{il}\right|^2\right\}\\ &= \mathbb{E}\left\{\mathbf{h}_{kl}^H\hat{\mathbf{h}}_{kl}\left(\mathbf{h}_{kl}^H\hat{\mathbf{h}}_{kl}\right)^H\right\}\\ &= \mathbb{E}\left\{\left(\hat{\mathbf{h}}_{kl}+\tilde{\mathbf{h}}_{kl}\right)^H\hat{\mathbf{h}}_{kl}\hat{\mathbf{h}}_{kl}^H\left(\hat{\mathbf{h}}_{kl}+\tilde{\mathbf{h}}_{kl}\right)\right\}\\ &= \mathbb{E}\left\{\hat{\mathbf{h}}_{kl}^H\hat{\mathbf{h}}_{kl}\hat{\mathbf{h}}_{kl}^H\hat{\mathbf{h}}_{kl}\right\} + \mathbb{E}\left\{\mathrm{tr}(\hat{\mathbf{h}}_{kl}\hat{\mathbf{h}}_{kl}^H\tilde{\mathbf{h}}_{kl}\tilde{\mathbf{h}}_{kl}^H)\right\}\\ &= \mathbb{E}\left\{\left\|\hat{\mathbf{h}}_{kl}\right\|^4\right\} + \mathrm{tr}\left(\mathbf{U}_{kl}\boldsymbol{\Psi}_{t_kl}^{-1}\mathbf{U}_{kl}\mathbf{C}_{kl}\right)\\ &= \mathbb{E}\left\{\left\|\hat{\mathbf{h}}_{kl}\right\|^4\right\} + \mathrm{tr}\left(\mathbf{U}_{kl}\boldsymbol{\Psi}_{t_kl}^{-1}\mathbf{U}_{kl}\left(\mathbf{R}_{kl}-\mathbf{U}_{kl}\boldsymbol{\Psi}_{t_kl}^{-1}\mathbf{U}_{kl}\right)\right)\\ &= \mathrm{tr}\left(\mathbf{U}_{kl}\boldsymbol{\Psi}_{t_kl}^{-1}\mathbf{U}_{kl}\mathbf{R}_{kl}\right) + \mathbb{E}\left\{\left\|\hat{\mathbf{h}}_{kl}\right\|^4\right\} - \mathrm{tr}\left(\left[\mathbf{U}_{kl}\boldsymbol{\Psi}_{t_kl}^{-1}\mathbf{U}_{kl}\right]^2\right)\end{aligned} \tag{B.3}$$

2) If $i \neq k$,

$$\begin{aligned}&\mathbb{E}\left\{\left|\mathbf{h}_{kl}^H\hat{\mathbf{h}}_{il}\right|^2\right\} = \mathbb{E}\left\{\mathbf{h}_{kl}^H\hat{\mathbf{h}}_{il}\left(\mathbf{h}_{kl}^H\hat{\mathbf{h}}_{il}\right)^H\right\}\\ &= \mathrm{tr}\left(\mathbb{E}\left\{\hat{\mathbf{h}}_{il}\hat{\mathbf{h}}_{il}^H\right\}\mathbb{E}\left\{\mathbf{h}_{kl}\mathbf{h}_{kl}^H\right\}\right)\\ &= \mathrm{tr}\left(\mathbb{E}\left\{\mathbf{U}_{il}\boldsymbol{\Psi}_{t_il}^{-1}\mathbf{y}_{t_il}^p\left(\mathbf{U}_{il}\boldsymbol{\Psi}_{t_il}^{-1}\mathbf{y}_{t_il}^p\right)^H\right\}\mathbf{R}_{kl}\right)\\ &= \mathrm{tr}\left(\mathbf{U}_{il}\boldsymbol{\Psi}_{t_il}^{-1}\mathbb{E}\left\{\mathbf{y}_{t_il}^p\left(\mathbf{y}_{t_il}^p\right)^H\right\}\left(\mathbf{U}_{il}\boldsymbol{\Psi}_{t_il}^{-1}\right)^H\mathbf{R}_{kl}\right)\\ &= \mathrm{tr}\left(\mathbf{U}_{il}\boldsymbol{\Psi}_{t_il}^{-1}\mathbf{U}_{il}\mathbf{R}_{kl}\right)\end{aligned} \tag{B.4}$$

Finally, substituting (B.2), (B.3) and (B.4) into (B.1), we can obtain (11).

APPENDIX C
A APPLICATION EXAMPLE OF ALGORITHM 1

Here, we consider a special case of cell-free mMIMO, that is, the number of users $K = 2$, the number of APs $L = 2$, and the number of AP antennas $N = 2$. Then the downlink power optimization problem in (21) can be expressed as follows,

$$\begin{aligned}&\min_{p_{il}}\ P_{total} = \sum_{l=1}^{2}\frac{1}{\alpha_l}\sum_{i=1}^{2}p_{il}\eta_{il}\\ &s.t.\ \sum_{l=1}^{2}p_{kl}\left(\frac{\eta_{kl}^2}{\tilde{\mu}_k}-\chi_{kl}\right)\\ &\quad-\sum_{i=1}^{2}\sum_{l=1}^{2}p_{il}\xi_{k,i,l}-\sigma_k^2\geq 0\quad k=1,2\\ &\quad\gamma_{l,n}-\frac{1}{\alpha_l}\sum_{i=1}^{2}p_{il}g_{i,l,n}\geq 0\ \ l=1,2,n=1,2\end{aligned} \tag{C.1}$$

$$\begin{aligned}\mathrm{SE}_k^d &= \sum_{j=1}^{L}\mathrm{SE}_{kj}^d = \sum_{j=1}^{L}\frac{\tau_d}{\tau_c}\log_2\left(1+\mathrm{SINR}_{kj}^d\right)\\ &= \frac{\tau_d}{\tau_c}\log_2\left(\prod_{J=1}^{L}\left(1+\mathrm{SINR}_{kj}^d\right)\right)\\ &= \frac{\tau_d}{\tau_c}\log_2\left(\prod_{j=1}^{L}\left(1+\frac{p_{kj}\left|\mathbb{E}\left\{\mathbf{h}_{kj}^H\mathbf{w}_{kj}\right\}\right|^2}{\sum_{i=1}^{K}\sum_{l=1}^{L}p_{il}\mathbb{E}\left\{\left|\mathbf{h}_{kl}^H\mathbf{w}_{il}\right|^2\right\}-\sum_{l=1}^{j}p_{kl}\mathbb{E}\left\{\left|\mathbf{h}_{kl}^H\mathbf{w}_{kl}\right|^2\right\}+\sigma_k^2}\right)\right)\\ &= \frac{\tau_d}{\tau_c}\log_2\left(1+\frac{\sum_{l=1}^{L}p_{kl}\left|\mathbb{E}\left\{\mathbf{h}_{kl}^H\mathbf{w}_{kl}\right\}\right|^2}{\sum_{i=1}^{K}\sum_{l=1}^{L}p_{il}\mathbb{E}\left\{\left|\mathbf{h}_{kl}^H\mathbf{w}_{il}\right|^2\right\}-\sum_{l=1}^{L}p_{kl}\left|\mathbb{E}\left\{\mathbf{h}_{kl}^H\mathbf{w}_{kl}\right\}\right|^2+\sigma_k^2}\right)\end{aligned} \tag{A.4}$$

By using LM method [17], the above optimization problems can be converted to

$$\mathcal{L}(p,\lambda,\mu)=\sum_{l=1}^{2}\frac{1}{\alpha_l}\sum_{i=1}^{2}p_{il}\eta_{il}+\sum_{k=1}^{2}\lambda_k\left(\sum_{l=1}^{2}p_{kl}\left(\frac{\eta_{kl}^2}{\tilde{\mu}_k}-\chi_{kl}\right)-\sum_{i=1}^{2}\sum_{l=1}^{2}p_{il}\xi_{k,i,l}-\sigma_k^2\right)+\sum_{l=1}^{2}\sum_{n=1}^{2}\mu_{l,n}\left(\gamma_{l,n}-\frac{1}{\alpha_l}\sum_{i=1}^{2}p_{il}g_{i,l,n}\right) \tag{C.2}$$

where λ,μ are LMs. By calculating the partial derivative of (C.2), we can obtain the KKT conditions:

$$\frac{\partial L}{\partial p_{11}}=\frac{1}{\alpha_1}\eta_{11}+\lambda_1\left(\frac{\eta_{11}^2}{\tilde{\mu}_1}-\chi_{11}\right)-\sum_{k=1}^{2}\lambda_k\xi_{k,1,1}-\frac{1}{\alpha_1}\sum_{n=1}^{2}\mu_{1,n}g_{1,1,n}\geq 0\quad \text{if } p_{11}^*\geq 0 \tag{C.3}$$

$$\frac{\partial L}{\partial p_{12}}=\frac{1}{\alpha_2}\eta_{12}+\lambda_1\left(\frac{\eta_{12}^2}{\tilde{\mu}_1}-\chi_{12}\right)-\sum_{k=1}^{2}\lambda_k\xi_{k,1,2}-\frac{1}{\alpha_2}\sum_{n=1}^{2}\mu_{2,n}g_{1,2,n}\geq 0\quad \text{if } p_{12}^*\geq 0 \tag{C.4}$$

$$\frac{\partial L}{\partial p_{21}}=\frac{1}{\alpha_1}\eta_{21}+\lambda_2\left(\frac{\eta_{21}^2}{\tilde{\mu}_1}-\chi_{21}\right)-\sum_{k=1}^{2}\lambda_k\xi_{k,2,1}-\frac{1}{\alpha_1}\sum_{n=1}^{2}\mu_{1,n}g_{2,1,n}\geq 0\quad \text{if } p_{21}^*\geq 0 \tag{C.5}$$

$$\frac{\partial L}{\partial p_{22}}=\frac{1}{\alpha_2}\eta_{22}+\lambda_2\left(\frac{\eta_{22}^2}{\tilde{\mu}_1}-\chi_{22}\right)-\sum_{k=1}^{2}\lambda_k\xi_{k,2,2}-\frac{1}{\alpha_2}\sum_{n=1}^{2}\mu_{2,n}g_{2,2,n}\geq 0\quad \text{if } p_{22}^*\geq 0 \tag{C.6}$$

$$\frac{\partial L}{\partial \lambda_1}=\sum_{l=1}^{2}p_{1l}\left(\frac{\eta_{1l}^2}{\tilde{\mu}_1}-\chi_{1l}\right)-\sum_{i=1}^{2}\sum_{l=1}^{2}p_{il}\xi_{1,i,l}-\sigma_1^2\geq 0\quad \text{if } \lambda_1^*\geq 0 \tag{C.7}$$

$$\frac{\partial L}{\partial \lambda_2}=\sum_{l=1}^{2}p_{2l}\left(\frac{\eta_{2l}^2}{\tilde{\mu}_2}-\chi_{2l}\right)-\sum_{i=1}^{2}\sum_{l=1}^{2}p_{il}\xi_{2,i,l}-\sigma_2^2\geq 0\quad \text{if } \lambda_2^*\geq 0 \tag{C.8}$$

$$\frac{\partial L}{\partial \mu_{1,1}}=\gamma_{1,1}-\frac{1}{\alpha_1}\sum_{i=1}^{2}p_{i1}g_{i,1,1}\geq 0\ \text{ if }\ \mu_{1,1}^*\geq 0 \tag{C.9}$$

$$\frac{\partial L}{\partial \mu_{1,2}}=\gamma_{1,2}-\frac{1}{\alpha_1}\sum_{i=1}^{2}p_{i1}g_{i,1,2}\geq 0\ \text{ if }\ \mu_{1,2}^*\geq 0 \tag{C.10}$$

$$\frac{\partial L}{\partial \mu_{2,1}}=\gamma_{2,1}-\frac{1}{\alpha_2}\sum_{i=1}^{2}p_{i2}g_{i,2,1}\geq 0\ \text{ if }\ \mu_{2,1}^*\geq 0 \tag{C.11}$$

$$\frac{\partial L}{\partial \mu_{2,2}}=\gamma_{2,2}-\frac{1}{\alpha_2}\sum_{i=1}^{2}p_{i2}g_{i,2,2}\geq 0\ \text{ if }\ \mu_{2,2}^*\geq 0 \tag{C.12}$$

In order to obtain the optimal solution $p_{11},p_{12},p_{21},p_{22}$, we need to solve (C.3)-(C.12) separately. If λ,μ is positive, then their corresponding Lagrangian derivatives should be equal to zero. If the optimal solution $p_{11},p_{12},p_{21},p_{22}$ is positive, then their corresponding Lagrange derivatives should also be equal to zero. Since there are only four unknowns, only four equations are needed to solve downlink power $p_{11},p_{12},p_{21},p_{22}$. Then for (C.7)-(C.12), and there must be four inequalities to take zero. The remaining two inequalities can be used as constraints to verify the optimal solution.

By solving any four equations in (C.7)-(C.12), we can get the optimal power solution $p_{11},p_{12},p_{21},p_{22}$. Then (C.3)-(C.6) can solve the required LMs, and further verify the optimal solution.

APPENDIX D
PROOF OF (29)

In order to get (29) from (28), we need to calculate $|\mathrm{DS}_k|^2$, $\mathbb{E}\left\{|\mathrm{BU}_k|^2\right\}$ and $\sum_{i\neq k}^{K}\mathbb{E}\left\{|\mathrm{UI}_{ki}|^2\right\}$ respectively.

$$|\mathrm{DS}_k|^2=\left|\mathbb{E}\left\{\sum_{l=1}^{L}\sqrt{p_{kl}}\mathbf{h}_{kl}^H\mathbf{w}_{kl}\right\}\right|^2 \tag{D.1}$$

$$\mathbb{E}\left\{|\mathrm{BU}_k|^2\right\}=\mathbb{E}\left\{\left|\sum_{l=1}^{L}\sqrt{p_{kl}}\mathbf{h}_{kl}^H\mathbf{w}_{kl}-\mathbb{E}\left\{\sum_{l=1}^{L}\sqrt{p_{kl}}\mathbf{h}_{kl}^H\mathbf{w}_{kl}\right\}\right|^2\right\}=\mathbb{E}\left\{\left|\sum_{l=1}^{L}\sqrt{p_{kl}}\mathbf{h}_{kl}^H\mathbf{w}_{kl}\right|^2\right\}-\left|\mathbb{E}\left\{\sum_{l=1}^{L}\sqrt{p_{kl}}\mathbf{h}_{kl}^H\mathbf{w}_{kl}\right\}\right|^2 \tag{D.2}$$

$$\sum_{i\neq k}^{K}\mathbb{E}\left\{|\mathrm{UI}_{ki}|^2\right\}=\sum_{i\neq k}^{K}\mathbb{E}\left\{\left|\sum_{l=1}^{L}\sqrt{p_{il}}\mathbf{h}_{kl}^H\mathbf{w}_{il}\right|^2\right\}=\sum_{i=1}^{K}\mathbb{E}\left\{\left|\sum_{l=1}^{L}\sqrt{p_{il}}\mathbf{h}_{kl}^H\mathbf{w}_{il}\right|^2\right\}-\mathbb{E}\left\{\left|\sum_{l=1}^{L}\sqrt{p_{kl}}\mathbf{h}_{kl}^H\mathbf{w}_{kl}\right|^2\right\} \tag{D.3}$$

Then, substituting (D.1), (D.2), and (D.3) into (28), we can obtain (29).

APPENDIX E
PROOF OF THEOREM 2

By substituting $\mathbf{w}_{kl} = \hat{\mathbf{h}}_{kl}$ into (29), we can get

$$\mathrm{SINR}_k^d = \frac{\left|\mathbb{E}\left\{\sum_{l=1}^{L}\sqrt{p_{kl}}\mathbf{h}_{kl}^H\hat{\mathbf{h}}_{kl}\right\}\right|^2}{\sum_{i=1}^{K}\mathbb{E}\left\{\left|\sum_{l=1}^{L}\sqrt{p_{il}}\mathbf{h}_{kl}^H\hat{\mathbf{h}}_{il}\right|^2\right\}-\left|\mathbb{E}\left\{\sum_{l=1}^{L}\sqrt{p_{kl}}\mathbf{h}_{kl}^H\hat{\mathbf{h}}_{kl}\right\}\right|^2+\sigma_k^2} \tag{E.1}$$

For the numerator term in (E.1), we can get

$$\begin{aligned}\left|\mathbb{E}\left\{\sum_{l=1}^{L}\sqrt{p_{kl}}\mathbf{h}_{kl}^H\mathbf{w}_{kl}\right\}\right|^2 &= \left|\sum_{l=1}^{L}\sqrt{p_{kl}}\mathbb{E}\left\{\mathbf{h}_{kl}^H\hat{\mathbf{h}}_{kl}\right\}\right|^2\\ &= \left|\sum_{l=1}^{L}\sqrt{p_{kl}}\mathrm{tr}\left(\mathbb{E}\left\{\mathbf{U}_{kl}\boldsymbol{\Psi}_{t_kl}^{-1}\mathbf{y}_{t_kl}^p\mathbf{h}_{kl}^H\right\}\right)\right|^2\\ &= \left|\sum_{l=1}^{L}\sqrt{p_{kl}}\mathrm{tr}\left(\mathbf{U}_{kl}\boldsymbol{\Psi}_{t_kl}^{-1}\mathbf{U}_{kl}\right)\right|^2\end{aligned} \tag{E.2}$$

Then, for the first denominator term in (E.1), we need to discuss in two cases.

1) If $i = k$,

$$\begin{aligned}\mathbb{E}\left\{\left|\sum_{l=1}^{L}\sqrt{p_{il}}\mathbf{h}_{kl}^H\hat{\mathbf{h}}_{il}\right|^2\right\} &= \mathbb{E}\left\{\left|\sum_{l=1}^{L}\sqrt{p_{kl}}\left(\hat{\mathbf{h}}_{kl}^H+\tilde{\mathbf{h}}_{kl}^H\right)\hat{\mathbf{h}}_{kl}\right|^2\right\}\\ &= \mathbb{E}\left\{\sum_{l_1=1}^{L}\sum_{l_2=1}^{L}\sqrt{p_{kl_1}p_{kl_2}}\hat{\mathbf{h}}_{kl_1}^H\hat{\mathbf{h}}_{kl_1}\hat{\mathbf{h}}_{kl_2}^H\hat{\mathbf{h}}_{kl_2}\right\}\\ &\quad+\mathbb{E}\left\{\sum_{l=1}^{L}p_{kl}\tilde{\mathbf{h}}_{kl}^H\hat{\mathbf{h}}_{kl}\hat{\mathbf{h}}_{kl}^H\tilde{\mathbf{h}}_{kl}\right\}\\ &= \left|\sum_{l=1}^{L}\sqrt{p_{kl}}\mathrm{tr}\left(\mathbf{U}_{kl}\left(\boldsymbol{\Psi}_{t_kl}^{-1}\right)^H\mathbf{U}_{kl}^H\right)\right|^2+\sum_{l=1}^{L}p_{kl}\mathbb{E}\left\{\left\|\hat{\mathbf{h}}_{kl}\right\|^4\right\}\\ &\quad-\sum_{l=1}^{L}p_{kl}\left[\mathrm{tr}\left(\mathbf{U}_{kl}\boldsymbol{\Psi}_{t_kl}^{-1}\mathbf{U}_{kl}\right)\right]^2\\ &\quad+\sum_{l=1}^{L}p_{kl}\mathrm{tr}\left[\mathbf{U}_{kl}\left(\boldsymbol{\Psi}_{t_kl}^{-1}\right)^H\mathbf{U}_{kl}^H\mathbf{C}_{kl}\right]\\ &= \sum_{l=1}^{L}p_{kl}\mathrm{tr}\left(\mathbf{U}_{kl}\boldsymbol{\Psi}_{t_kl}^{-1}\mathbf{U}_{kl}\mathbf{R}_{kl}\right)+\left|\sum_{l=1}^{L}\sqrt{p_{kl}}\mathrm{tr}\left(\mathbf{U}_{kl}\boldsymbol{\Psi}_{t_kl}^{-1}\mathbf{U}_{kl}\right)\right|^2\\ &\quad+\sum_{l=1}^{L}p_{kl}\mathbb{E}\left\{\left\|\hat{\mathbf{h}}_{kl}\right\|^4\right\}-\sum_{l=1}^{L}p_{kl}\left[\mathrm{tr}\left(\mathbf{U}_{kl}\boldsymbol{\Psi}_{t_kl}^{-1}\mathbf{U}_{kl}\right)\right]^2\\ &\quad-\sum_{l=1}^{L}p_{kl}\mathrm{tr}\left(\left(\mathbf{U}_{kl}\boldsymbol{\Psi}_{t_kl}^{-1}\mathbf{U}_{kl}\right)^2\right)\end{aligned} \tag{E.3}$$

2) If $i \neq k$,

$$\begin{aligned}\mathbb{E}\left\{\left|\sum_{l=1}^{L}\sqrt{p_{il}}\mathbf{h}_{kl}^H\hat{\mathbf{h}}_{il}\right|^2\right\} &= \mathbb{E}\left\{\sum_{l=1}^{L}p_{il}\mathbf{h}_{kl}^H\hat{\mathbf{h}}_{il}\hat{\mathbf{h}}_{il}^H\mathbf{h}_{kl}\right\}\\ &= \sum_{l=1}^{L}p_{il}\mathrm{tr}\left(\mathbb{E}\left\{\hat{\mathbf{h}}_{il}\hat{\mathbf{h}}_{il}^H\right\}\mathbb{E}\left\{\mathbf{h}_{kl}\mathbf{h}_{kl}^H\right\}\right)\\ &= \sum_{l=1}^{L}p_{il}\mathrm{tr}\left(\mathbb{E}\left\{\mathbf{U}_{il}\boldsymbol{\Psi}_{t_il}^{-1}\mathbf{y}_{t_il}^p\left(\mathbf{U}_{il}\boldsymbol{\Psi}_{t_il}^{-1}\mathbf{y}_{t_il}^p\right)^H\right\}\mathbf{R}_{kl}\right)\\ &= \sum_{l=1}^{L}p_{il}\mathrm{tr}\left(\mathbf{U}_{il}\boldsymbol{\Psi}_{t_il}^{-1}\mathbf{U}_{il}\mathbf{R}_{kl}\right)\end{aligned} \tag{E.4}$$

Finally, substituting (E.2), (E.3) and (E.4) into (E.1), we can obtain (30).

REFERENCES

[1] H. Q. Ngo, E. G. Larsson, and T. L. Marzetta, "Energy and spectral efficiency of very large multiuser MIMO systems," *IEEE Trans. Commun.*, vol. 61, no. 4, pp. 1436–1449, Apr. 2013.
[2] E. G. Larsson, O. Edfors, F. Tufvesson, and T. L. Marzetta, "Massive MIMO for next generation wireless systems," *IEEE Commun. Mag.*, vol. 52, no. 2, pp. 186–195, Feb. 2014.
[3] J. Ma, S. Zhang, H. Li, N. Zhao, and V. C. M. Leung, "Interference-alignment and soft-space-reuse based cooperative transmission for multi-cell massive MIMO networks," *IEEE Trans. Wireless Commun.*, vol. 17, no. 3, pp. 1907–1922, Mar. 2018.
[4] G. Interdonato, E. Björnson, H. Q. Ngo, P. Frenger, and E. G. Larsson, "Ubiquitous cell-free massive MIMO communications," *EURASIP J. Wireless Commun. Netw.*, vol. 2019, no. 1, pp. 1–19, Dec. 2019.
[5] H. Q. Ngo, A. Ashikhmin, H. Yang, E. G. Larsson, and T. L. Marzetta, "Cell-free massive MIMO versus small cells," *IEEE Trans. Wireless Commun.*, vol. 16, no. 3, pp. 1834–1850, Mar. 2017.
[6] J. Zhang, S. Chen, Y. Lin, J. Zheng, B. Ai, and L. Hanzo, "Cell-free massive MIMO: A new next-generation paradigm," *IEEE Access*, vol. 7, pp. 99878–99888, 2019.
[7] E. Bjornson and L. Sanguinetti, "Making cell-free massive MIMO competitive with MMSE processing and centralized implementation," *IEEE Trans. Wireless Commun.*, vol. 19, no. 1, pp. 77–90, Jan. 2020.
[8] N. Zhao, F. R. Yu, and H. Sun, "Adaptive energy-efficient power allocation in green interference-alignment-based wireless networks," *IEEE Trans. Veh. Technol.*, vol. 64, no. 9, pp. 4268–4281, Sep. 2015.
[9] H. Q. Ngo, L.-N. Tran, T. Q. Duong, M. Matthaiou, and E. G. Larsson, "On the total energy efficiency of cell-free massive MIMO," *IEEE Trans. Green Commun. Netw.*, vol. 2, no. 1, pp. 25–39, Mar. 2018.
[10] L. D. Nguyen, T. Q. Duong, H. Q. Ngo, and K. Tourki, "Energy efficiency in cell-free massive MIMO with zero-forcing precoding design," *IEEE Commun. Lett.*, vol. 21, no. 8, pp. 1871–1874, Aug. 2017.
[11] J. Zhang, Y. Wei, E. Bjornson, Y. Han, and X. Li, "Spectral and energy efficiency of cell-free massive MIMO systems with hardware impairments," in *Proc. 9th Int. Conf. Wireless Commun. Signal Process. (WCSP)*, Nanjing, China, Oct. 2017, pp. 1–6.
[12] M. Alonzo, S. Buzzi, and A. Zappone, "Energy-efficient downlink power control in mmWave cell-free and user-centric massive MIMO," in *Proc. IEEE 5G World Forum (5GWF)*, Jul. 2018, pp. 493–496.
[13] M. Alonzo and S. Buzzi, "Cell-free and user-centric massive MIMO at millimeter wave frequencies," in *Proc. IEEE 28th Annu. Int. Symp. Pers., Indoor, Mobile Radio Commun. (PIMRC)*, Oct. 2017, pp. 1–5.
[14] H. Yang and T. L. Marzetta, "Energy efficiency of massive MIMO: Cell-free vs. cellular," in *Proc. IEEE 87th Veh. Technol. Conf. (VTC Spring)*, Jun. 2018, pp. 1–5.
[15] M. Attarifar, A. Abbasfar, and A. Lozano, "Modified conjugate beamforming for cell-free massive MIMO," *IEEE Wireless Commun. Lett.*, vol. 8, no. 2, pp. 616–619, Apr. 2019.
[16] E. Björnson, J. Hoydis, and L. Sanguinetti, "Massive MIMO networks: Spectral, energy, and hardware efficiency," *Found. Trends Signal Process.*, vol. 11, nos. 3–4, pp. 154–655, 2017.
[17] S. Boyd and L. Vandenberghe, *Convex Optimization*. Cambridge, U.K.: Cambridge Univ. Press, 2004.
[18] *Coordinated Multi-Point Operation for LTE Physical Layer Aspects*, document TR 36.819, 3GPP, Sep. 2011.
[19] *Discussions on DL CoMP Schemes*, document TSG-RAN WG1 66 R1-113353, 3GPP, Ericsson, Oct. 2011.
[20] R. Tanbourgi, S. Singh, J. G. Andrews, and F. K. Jondral, "Analysis of non-coherent joint-transmission cooperation in heterogeneous cellular networks," in *Proc. IEEE Int. Conf. Commun. (ICC)*, Jun. 2014.

[21] O. Ozdogan, E. Bjornson, and J. Zhang, "Performance of cell-free massive MIMO with Rician fading and phase shifts," *IEEE Trans. Wireless Commun.*, vol. 18, no. 11, pp. 5299–5315, Nov. 2019.
[22] T. Van Chien, E. Bjornson, and E. G. Larsson, "Joint power allocation and user association optimization for massive MIMO systems," *IEEE Trans. Wireless Commun.*, vol. 15, no. 9, pp. 6384–6399, Sep. 2016.
[23] D. Tse and P. Viswanath, *Fundamentals of Wireless Communication*. Cambridge, U.K.: Cambridge Univ. Press, 2005.
[24] W. Yu and T. Lan, "Transmitter optimization for the multi-antenna downlink with per-antenna power constraints," *IEEE Trans. Signal Process.*, vol. 55, no. 6, pp. 2646–2660, Jun. 2007.
[25] H. Dahrouj and W. Yu, "Coordinated beamforming for the multicell multi-antenna wireless system," *IEEE Trans. Wireless Commun.*, vol. 9, no. 5, pp. 1748–1759, May 2010.
[26] M. S. Ali, H. Tabassum, and E. Hossain, "Dynamic user clustering and power allocation for uplink and downlink non-orthogonal multiple access (NOMA) systems," *IEEE Access*, vol. 4, pp. 6325–6343, 2016.
[27] CVX Research. (2020). *CVX: MATLAB Software for Disciplined Convex Programming, Version 2.2*. [Online]. Available: http://cvxr.com/cvx

JIAHUA QIU was born in 1993. He received the B.E. degree from the PLA University of Science and Technology, in 2014. He is currently pursuing the M.S. degree with the Institution of Communications Engineering, Army Engineering University of PLA. His research interests include MIMO techniques and cell-free massive MIMO.

KUI XU (Member, IEEE) was born in 1982. He received the B.E. degree in wireless communications and the Ph.D. degree in software defined radio from the PLA University of Science and Technology, Nanjing, China, in 2004 and 2009, respectively.

He is currently an Associate Professor with the College of Communications Engineering, Army Engineering University of PLA. He has authored about 100 articles in refereed journals and conference proceedings. He holds five patents in China. His research interests include broadband wireless communications, signal processing for communications, network coding, and wireless communication networks. He has served on the Technical Program Committee of the IEEE WCSP2014, WCSP2015, ICSPDM2015, and SIRS2015 TPC. He received the URSI Young Scientists Award, in 2014, and the 2010 Ten Excellent Doctor Degree Dissertation Award of PLAUST. He serves as a Reviewer of the IEEE TRANSACTIONS ON WIRELESS COMMUNICATION, the IEEE TRANSACTIONS ON VEHICLE TECHNOLOGY, the IEEE COMMUNICATIONS LETTERS, and the IEEE SIGNAL PROCESSING LETTERS.

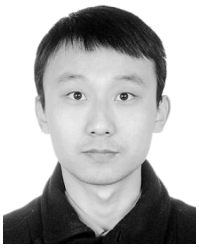

XIAOCHEN XIA was born in China, 1987. He received the B.E. degree in electronic science and technology from Tianjin University (TJU), in 2010, and the Ph.D. degree in communication and information system from the PLA University of Science and Technology, in 2017. His research interests include relaying networks, full-duplex communication, network coding, and MIMO techniques. He received the 2013 Excellent Master Degree Dissertation Award of Jiangsu Province, China.

ZHEXIAN SHEN was born in 1993. He received the B.E. degree in communications engineering from the Nanjing University of Posts and Telecommunications, in 2016. He is currently pursuing the Ph.D. degree with the Institution of Communications Engineering, Army Engineering University of PLA. His research interests include MIMO techniques, heterogeneous networks, full-duplex communication, and network coding.

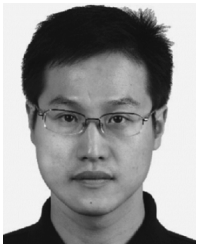

WEI XIE was born in 1977. He received the B.E. degree in microwave communication from the Institute of Communications Engineering, Nanjing, China, in 1999, and the M.S. degree in communications and information system from the PLA University of Science and Technology, Nanjing, in 2002. He is currently an Associate Professor with the College of Communications Engineering, Army Engineering University of PLA. His research interests include broadband wireless communications, signal processing for communications, network coding, and wireless communication networks.